Coherent exchange-coupled nonlocal Kondo impurities

Lidia Stocker [1,*] and Oded Zilberberg [2]

[1]*Institute for Theoretical Physics, ETH Zurich, 8093 Zurich, Switzerland*
[2]*Department of Physics, University of Konstanz, 78457 Konstanz, Germany*

Quantum dots exhibit a variety of strongly correlated effects, e.g., they can emulate localized magnetic impurities that form a Kondo singlet with their surrounding environment. Interestingly, in double-dot setups, such magnetic impurities couple to each other by direct Ruderman-Kittel-Kasuya-Yosida (RKKY) interaction, which wins over the Kondo physics. In this work, we investigate a double-dot device where the dots are coupled via off-resonant ballistic modes, dubbed electronic cavity modes. Within this cavity-double-dot system, we study, using variational matrix product state techniques, the competition between Kondo formation and the combined coherent orbital hybridization and RKKY-like interaction that the cavity facilitates. Specifically, we find that Kondo can form on each dot individually whereby the cavity can either (i) destroy the Kondo via the RKKY that mediates a singlet state on the two dots, or (ii) lead to an exotic orbital macrsoscopic superposition of the Kondo forming on each of the dots. We dub the latter "Kondo cat". En route to this key finding, we rigorously study the many-body phase diagram of the system, as well as compare it with the case of coupling the dots via an incoherent RKKY channel. The realization of a Kondo cat can facilitate applications in metrology, and reveal the spin coherence length in mesoscopic devices.

Introduction. The study of quantum dot systems draws continuous activity in condensed matter physics due to their potential applications in quantum information processing [1,2] and their tunable ability to explore strongly correlated effects [3,4]. A prominent example of strongly correlated physics in quantum dots is the Kondo effect [5]. It manifests when a dot's electron acts as a spin-degenerate magnetic impurity that is screened by the surrounding environment, leading to the formation of a macroscopic dot-environment spin singlet [3,6–8]. Apart from Kondo-like effects, double-dot systems are interesting due to the Ruderman-Kittel-Kasuya-Yosida (RKKY) interaction, which mediates effective coupling between distant impurities [9–11]. Combined, the two opposing effects compete: the Kondo effect tends to screen local moments and the RKKY interaction tends to order local moments. Understanding this competition holds immense implications for comprehending correlated electron systems and has been widely investigated in a variety of systems [12–20].

The RKKY interaction can also serve as a knob for quantum applications [21]. Here, one seeks to coherently control the spin states of the dots and implement local quantum operations, while keeping the ability to transfer quantum information between the system's building blocks. To this end, it is useful to keep the quantum dots separate in order to allow for precise control and manipulation of their individual properties [22]. Note, however, that in separated double dot systems, the central separating lead harbors partially suppressed RKKY interaction that coexists with a superexchange interaction [23]. This complicates its harnessing as a coherent entanglement bus. As such, there is a variety of alternative proposals for coupling distant dots, e.g., via the edge modes of the quantum Hall effect [24–26], using superconducting cavities [27–32], or replacing the central lead with a large, yet interacting dot [33].

Interestingly, coherent coupling between distant dots was experimentally achieved using a large open dot that has a structured density of states [34]. The structure harbors ballistic whispering gallery (standing) modes that are embedded in the larger expanse of states in the system [35–38], akin to quantum corrals [39,40]. We dub the standing modes appearing in the experiment *electronic cavity states*. The cavity modes are taken as a discrete set of spin degenerate levels due to screening in the large expanse of the device [36]. The first experimental realization of an electronic cavity coupled to a single dot showed a competition between a "molecular" dot-cavity singlet formation and the Kondo effect [35,36,41]. These results laid the foundation for employing all-electronic dot-cavity devices in quantum information processing applications and as a platform for the fundamental study of strongly correlated physics.

In this work, we comprehensively study the cavity-mediated strongly correlated states in a separated double-dot device. We observe the emergence of both RKKY-like interactions between distant dots and a nonlocal superposition of spin-Kondo singlets in either of the dots. Our study involves tomography of the double dot system [41] based on exact numerical techniques. When possible, our results are
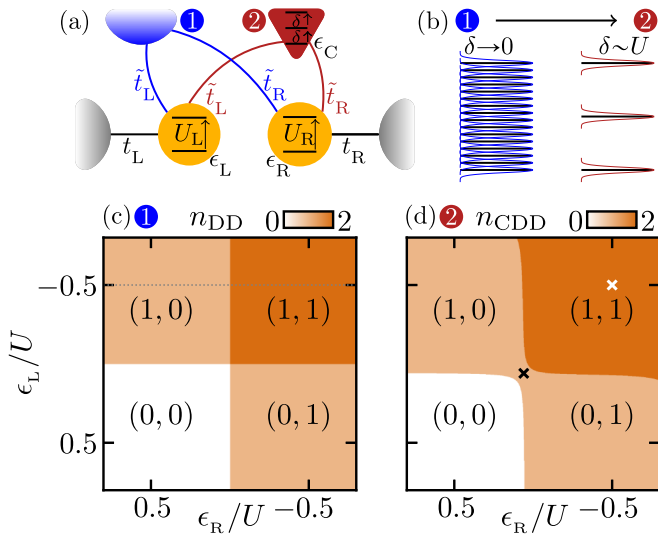
*Corresponding author: stocker@phys.ethz.ch

FIG. 1. *System and charge stability diagram.* (a) Double-dot system [cf. Eq. (1)] composed of two spinful single-level dots, $\ell \in L, R$ (yellow circle) with on-site energy ϵ_ℓ and interaction U_ℓ. They are tunnel-coupled (black lines) to their respective leads (gray semicircles) with tunneling amplitudes t_ℓ. The two dots are additionally tunnel-coupled (blue/red lines) to a central common lead with amplitudes $\tilde{t}_\ell$. (b) The central box has energy spacing δ with two limiting cases: (1, blue) a metallic lead when $\delta \to 0$, and (2, red) an electronic cavity when $\delta \sim U$. In reality [34], the electronic cavity is open, as depicted by broadened levels. (c) Charge stability diagram of the double-dot system (1). (d) Charge stability diagram of the cavity-double-dot system (2), where the cavity is truncated to a single-energy level $\epsilon_c = 0.75U$ ($\delta \to \infty$) for $\tilde{t}_D = 0.1U$. As the cavity is detuned from the Fermi level, its occupation is $n_c \approx 0$. The population of the two dots is marked by (n_L, n_R). The gray dotted line and white and black $\times$ mark the regions discussed below, see Figs. 2 and 3.

supported by analytical derivation of the double-dot system's configuration. First, we provide an exact solution to the interplay among Kondo, RKKY, and ferromagnetic interactions in a double-dot system coupled to a central continuous lead [23]. Next, we delve into the coherent physics that arises when the system is coupled to a detuned cavity. Here, we capture variants of the standard Kondo and RKKY effect, alongside predicting a fascinating nonlocal Kondo effect. Our results provide a comprehensive map of the many-body effects arising in separated double dots and inspire their experimental realization.

Model. Our double-dot system is composed of two Anderson impurity models [42], each coupled to its lead (environment) and a central common lead, see Fig. 1(a). Its effective model, derived in Ref. [36], reads

$$H = \sum_\ell \left(H_\ell + H_{\text{lead}}^\ell \right) + H_C^\delta + \sum_\ell \left(H_{\text{tun}}^{\text{lead}_\ell - \ell} + H_{\text{tun}}^{C - \ell} \right), \quad (1)$$

where $\ell \in \{L, R\}$ denotes the left and right dot. Each dot Hamiltonian $H_\ell = \sum_\sigma \epsilon_\ell n_{\ell\sigma} + U_\ell n_{\ell\uparrow} n_{\ell\downarrow}$ describes an impurity with a spin-degenerate electron level at energy ϵ_ℓ, and electron-electron charging energy U_ℓ. Here, $n_{\ell\sigma}$ denotes the dot level's occupation number with spin $\sigma \in \{\uparrow, \downarrow\}$. The

left and right leads are noninteracting continuous reservoirs $H_{\text{lead}}^\ell = \sum_{k\sigma} \epsilon_{k\ell} c_{k\ell\sigma}^\dagger c_{k\ell\sigma}$, where we denote $c_{k\ell\sigma}$ ($c_{k\ell\sigma}^\dagger$) as the fermionic annihilation (creation) of an electron with momentum k and spin σ in the ℓth lead. Each dot is coupled to its lead via $H_{\text{tun}}^{\text{lead}_\ell - \ell} = \sum_{\ell k\sigma} t_\ell d_\sigma^\dagger c_{k\ell\sigma} + \text{H.c.}$ with energy-independent tunneling amplitudes t_ℓ. We consider the central region as a set of noninteracting and equally spaced energy levels $H_C^\delta = \sum_{j\sigma} (\epsilon_C + j\delta) c_{j\sigma}^\dagger c_{j\sigma}$, where the fermionic operators $c_{j\sigma}$ ($c_{j\sigma}^\dagger$) are defined as those of the ℓ leads. The central region is tunnel-coupled to both dots $H_{\text{tun}}^{C - \ell} = \sum_{\ell j\sigma} \tilde{t}_\ell d_{\ell\sigma}^\dagger c_{j\sigma} + \text{H.c.}$ with energy-independent tunneling amplitudes $\tilde{t}_\ell$. In the following, for clarity, we consider identically tuned dots $U_\ell \equiv U, t_\ell \equiv t_D, \tilde{t}_\ell \equiv \tilde{t}_D$, and denote $\epsilon_\ell \equiv \epsilon_D$ whereas the dot's energy levels are equal. In the limit of vanishing level spacing $\delta \to 0$, denoted as system (1), the central region corresponds to a lead, see Fig. 1(b). In the situation where $\delta \sim U$, denoted as system (2), the levels of the central region are discrete and correspond to a multimode electronic cavity, used in the Kondo-box problem [43].

We start analyzing the charge stability diagram of the double-dot system in the limiting situations; (1) the separated double-dot system, and (2) the cavity-double-dot system, see Figs. 1(c) and 1(d). We assume that coupling to the leads is vanishing and exactly diagonalize the remaining "closed" impurity system. In case (1), for $t_D \approx \tilde{t}_D \approx 0$, the diagram of the closed two-dot system $H_{\text{DD}} = \sum_\ell H_\ell$, with $\langle n_{\text{DD}} \rangle = \langle n_L + n_R \rangle$, exhibits a standard Coulomb blockade on each of the dots individually, separated by "resonance lines" where the particle number on the double dot is ill defined. In case (2), the closed system is composed of the two dots and the discrete cavity levels. Here and in the following, we truncate and consider a cavity with a single energy level. Coupling the cavity to the dots, $\tilde{t}_D \neq 0$, we obtain an "artificial molecule" with Hamiltonian $H_{\text{CDD}} = \sum_\ell (H_\ell + H_{\text{tun}}^{C - \ell}) + H_C^\delta$, which for $|\tilde{t}_\ell| > 0$ creates avoided crossings as the levels with the same total number of electrons $\langle n_{\text{CDD}} \rangle = \langle n_C + n_L + n_R \rangle$ hybridize via the cavity.

Methodology. To analyze the many-body physics in our system, we calculate the "ground state" of the open system (impurity plus leads) using a numerical NRG-MPS method [41,44–49]. We consider the system at equilibrium (zero bias voltage $\mu_L = \mu_R = \mu_C$). We then trace out the leads and extract the elements of the double-dot impurity's reduced 16×16 density matrix, ρ_{DD}. The entirety of the 256 matrix elements collectively serve as a comprehensive descriptor (order parameters) for the type of strongly correlated states that form between the dots and their leads and can be probed using tomography methods [41]. In analytically treatable cases, we harness a Schrieffer-Wolff transformation (SWT) [50,51] to predict which values of ρ_{DD} mark which many-body state. In Table I, we summarize the values of the density matrix elements $|\langle s, s' | \rho_{\text{DD}} | s'', s''' \rangle|$ corresponding to the variety of effects (i)–(v) identified in this work [52], where $|s, s'\rangle = |s\rangle_L \otimes |s'\rangle_R$ and $s, s' \in \{0, \uparrow, \downarrow, \uparrow\downarrow\}$ denote the spin configuration of the left and right dot. The (i)–(v) effects are depicted in Fig. 2(a). Note that we apply the NRG-MPS tomography method to both cases (1) and (2). In the former, we introduce an additional lead to the environment by changing the NRG-MPS decomposition [52].
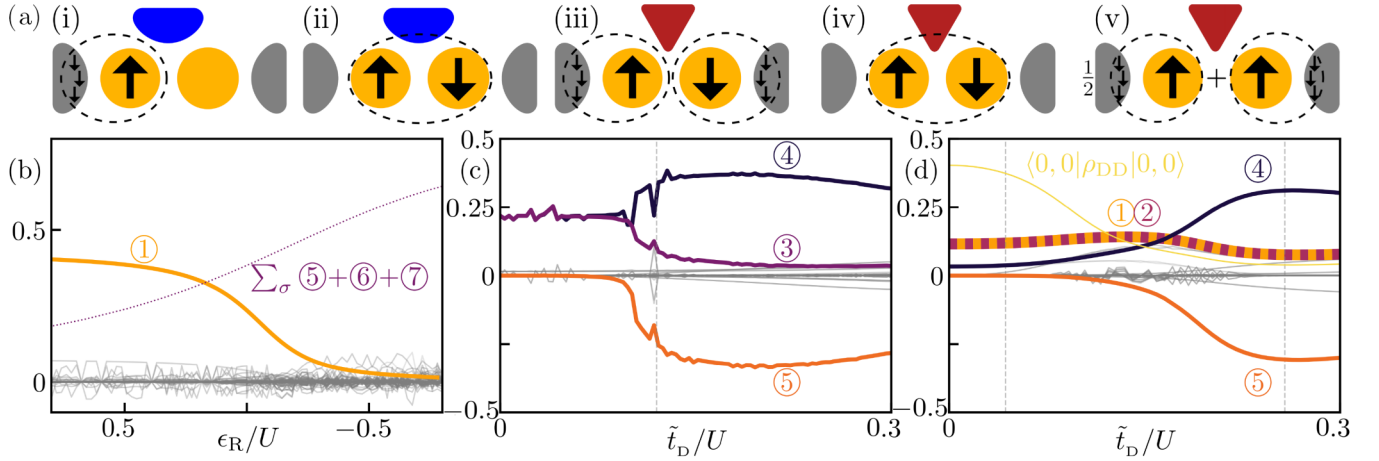
FIG. 2. *Crossovers between ground states.* (a) Competing hybridization mechanisms (dashed circle): (i) Standard spin Kondo between the left dot and its lead, (ii) dot-dot hybridization via the central lead, (iii) two separate dot-lead spin Kondo, (iv) cavity-mediated RKKY dot-dot singlet, and (v) Kondo cat. (b)–(d) NRG-MPS tomography results of the reduced double-dot impurity matrix elements $\langle s, s' | \rho_{\mathrm{DD}} | s'', s''' \rangle$. Out of the 256 matrix elements, we highlight those with a contribution $|\langle s, s' | \rho_{\mathrm{DD}} | s'', s''' \rangle| > 0.1$ and plot the other elements with thin gray lines. The circular numbered markers correspond to the elements in Table I. The line width represents the degeneracy of the configuration; onefold: thin, twofold: standard, fourfold: thick. (b) System (1) with $\epsilon_{\mathrm{L}} = -U/2$, $\tilde{t}_{\mathrm{D}} = 0.1$. Note that we sum over the (anti)ferromagnetic contributions (dotted line), cf. discussion in the main text. (c) System (2) with $\epsilon_{\mathrm{L}} = \epsilon_{\mathrm{R}} = -U/2$ [cf. white $\times$ in Fig. 1(d)] and $t_{\mathrm{D}} = 0.1U$. Gray line marks the boundary between the left region (where the Kondo gap dominates the RKKY gap) and the right region (where the RKKY gap dominates the Kondo gap). (d) System (2) with $\epsilon_{\mathrm{L}} = \epsilon_{\mathrm{R}} = 0.005U$ [cf. black $\times$ in Fig. 1(d)] and $t_{\mathrm{D}} = 0.1U$. Gray lines mark the regions with a different total number of electrons for the closed cavity-double-dot system, $n_{\mathrm{DD}} \approx 2, 1, 0$. We set the NRG chain length of each lead $N = 80$, the MPS bond dimension $D = 500$, and the leads are assumed to have a constant density of states $d_0 = 1/(2U)$.

Double-dot system; case (1). We first consider the case where $\epsilon_{\mathrm{L}} = -U/2$, and tune the level of the right dot ϵ_{R}, see Fig. 2(b). Here, the left dot is singly occupied, while the right moves from being empty to singly occupied, as ϵ_{R} decreases, cf. Fig. 1(c). For the double-dot impurity, our NRG-MPS tomography procedure produces 256 values. The configuration in the empty right dot region is a fingerprint for a Kondo singlet formation between the left dot and its lead, as predicted from standard SWT [3,52], cf. Table I and Fig. 2(ai). As the right dot becomes more occupied, the value of the order parameter $\langle 0, \sigma | \rho_{\mathrm{DD}} | 0, \sigma \rangle$ decreases, whereas the value of another order parameter $\sum_\sigma \langle \sigma, \sigma | \rho_{\mathrm{DD}} | \sigma, \sigma \rangle + \langle \sigma, \bar{\sigma} | \rho_{\mathrm{DD}} | \sigma, \bar{\sigma} \rangle + \langle \sigma, \bar{\sigma} | \rho_{\mathrm{DD}} | \bar{\sigma}, \sigma \rangle$ grows to become dominant and all the other matrix elements are close to zero. The resulting configuration in this region identifies dot-dot hybridization mediated by the central lead, where ferromagnetic superexchange coexists with antiferromagnetic RKKY-like interactions [23,52], cf. Fig. 2(aii). Note that we depict the

sum over the contributions of the (anti)ferromagnetic terms due to the degenerate ground state in the $\epsilon_{\mathrm{L}} < 0$ case [52]. Such a crossover was discussed analytically [53] and resembles the one observed experimentally in the case of a large central dot [33,54]. Here, we move beyond perturbative approaches and capture these effects (including the crossover between them) using a numerically exact method on the full (open) system. This is the first key result of our work.

Cavity-mediated RKKY; case (2). We consider now the cavity-double-dot system in the $\epsilon_{\mathrm{L}} = \epsilon_{\mathrm{R}} = -U/2$ regime (we henceforth consider the two dots with identical energy level ϵ_{D}), where both dots are singly occupied. In Fig. 2(c), we tune the dot-cavity coupling $\tilde{t}_{\mathrm{D}}$ and plot the tomography values. As $\tilde{t}_{\mathrm{D}}$ increases, the term $\langle \sigma, \bar{\sigma} | \rho_{\mathrm{DD}} | \sigma, \bar{\sigma} \rangle$ increases, while the term $\langle \sigma, \sigma | \rho_{\mathrm{DD}} | \sigma, \sigma \rangle$ decreases toward zero and the term $\langle \sigma, \bar{\sigma} | \rho_{\mathrm{DD}} | \bar{\sigma}, \sigma \rangle$ appears. The ρ_{DD} configuration for small $\tilde{t}_{\mathrm{D}}$ is the fingerprint of Kondo singlets forming between each dot and their respective lead independently, cf. Table I, and Fig. 2(aiii). As the first two terms gap out and the third term appears, we observe the fingerprint of a cavity-mediated singlet that forms on the two dots [52], cf. Table I and Fig. 2(aiv). Crucially, the singlet can be attributed to a "coherent RKKY interaction", unlike the standard RKKY mechanism that involves a continuum. Such coherent hybridization engenders a so-called exchange blockade [34], further distinguishing it from conventional RKKY behavior.

The formation of two separated Kondo effects opens a gap that is twice that of the Kondo gap for a single dot system [52]

TABLE I. Dot-dot density matrix $\langle s, s' | \rho_{\mathrm{DD}} | s'', s''' \rangle$ configuration corresponding to the (i)–(v) effects illustrated in Fig. 2(a), as calculated by exact diagonalization and SWT [52]. We omit the other 246 density matrix elements, as they are $= 0$ in (i)–(v).

	(i)	(ii)	(iii)	(iv)	(v)
① $\langle 0, \sigma | \rho_{\mathrm{DD}} | 0, \sigma \rangle$	0.5	0	0	0	0.25
② $\langle \sigma, 0 | \rho_{\mathrm{DD}} | \sigma, 0 \rangle$	0	0	0	0	0.25
③ $\langle \sigma, \sigma | \rho_{\mathrm{DD}} | \sigma, \sigma \rangle$	0		0.25	0	0
④ $\langle \sigma, \bar{\sigma} | \rho_{\mathrm{DD}} | \sigma, \bar{\sigma} \rangle$	0	$\sum = 1$	0.25	0.5	0
⑤ $\langle \sigma, \bar{\sigma} | \rho_{\mathrm{DD}} | \bar{\sigma}, \sigma \rangle$	0		0	−0.5	0

$$\Delta_{\text{2-Kondo}} = \sqrt{2\pi |t_{\mathrm{D}}|^2 U d_0} \exp\left(\frac{\epsilon_{\mathrm{D}}(\epsilon_{\mathrm{D}} + U)}{2|t_{\mathrm{D}}|^2 U d_0} \right), \quad (2)$$

where d_0 is the leads' density of states. Similarly, the dot-dot singlet formation opens a gap [52]

$$\Delta_{\text{RKKY}} \approx 48\tilde{t}_{\text{D}}^4/(U + 2\epsilon_{\text{C}})^3. \qquad (3)$$

The vertical gray line in Fig. 2(c) marks the critical $\tilde{t}_{\text{D}}$ value above which a dot-dot singlet formation is expected, as the RKKY dominates the Kondo gap $\Delta_{\text{RKKY}} > \Delta_{\text{2-Kondo}}$. This value is in good agreement with the crossover observed with our NRG-MPS results discussed above. A signature of such a dot-dot singlet formation was experimentally detected [34], with a theoretical description that was limited to the closed system. Here, we predict that the singlet can form in the realistic many-body setting and win against competing hybridization channels with the leads. It would be interesting to experimentally tune the cavity level ϵ_{C} in this detuned regime and observe the appearance of Kondo singlets. This is the second key result of our work; we numerically resolve the coherent long-range coupling between distant dots in the open cavity-double-dot system.

Kondo cat. As shown in Fig. 1(d), the coupling to the cavity opens a gap in the $\epsilon_{\text{D}} \approx 0$ region and the total occupation of the double dot system is $n_{\text{DD}} \approx 1$. We now set the dots' energy levels to $\epsilon_{\text{L}} = \epsilon_{\text{R}} = 0.005U$, and tune the dot-cavity coupling strength $\tilde{t}_{\text{D}}$, see Fig. 2(d). The empty-dot term $\langle 0, 0|\rho_{\text{DD}}|0, 0\rangle$ decreases toward zero for increasing dot-cavity coupling as the exchange gap opens and the dots become more occupied. Conversely, the term $\langle \sigma, \bar{\sigma}|\rho_{\text{DD}}|\sigma, \bar{\sigma}\rangle$ increases as both dots become singly occupied. In the midst of the parameter scan, terms with total double-dot occupation close to one $\langle 0, \sigma|\rho_{\text{DD}}|0, \sigma\rangle$ and $\langle \sigma, 0|\rho_{\text{DD}}|\sigma, 0\rangle$ are dominant.

To better understand this signature, we consider the hybridized orbits regime that appears around $\epsilon_{\text{D}} \approx 0$ and opens a gap [52]

$$\Delta_{\text{orb}} = 2\tilde{t}_{\text{D}}^2/(\epsilon_{\text{C}} - \epsilon_{\text{D}}), \qquad (4)$$

leading to $n_{\text{DD}} \approx 1$ for $\epsilon_{\text{D}} - \Delta_{\text{orb}} < \min(0, 2\epsilon_{\text{D}})$, when the energy is lower than the energy of the empty and doubly occupied states [in Fig. 2(d), this occurs within the vertical gray lines]. We find that the ground state of the dot-dot system in the $n_{\text{DD}} \approx 1$ configuration is spin degenerate and the nonlocal magnetic moment on either of the dots is screened by its respective lead [52]. Thus, the system is in a nonlocal orbital superposition of two macroscopic states: both describe a filled dot spin state that is screened by its lead (Kondo singlet) while the other dot is empty. We dub this configuration a "Kondo cat".

Our NRG-MPS tomography results capture such a Kondo cat formation in the midst of the $n_{\text{DD}} \approx 1$ regime, see Table I and Figs. 2(av) and 2(d). We note that the nonzero fingerprints for the Kondo cat are lower than the expected 0.25 value and the terms $\langle \sigma, \bar{\sigma}|\rho_{\text{DD}}|\sigma, \bar{\sigma}\rangle$, $\langle \sigma, \bar{\sigma}|\rho_{\text{DD}}|\bar{\sigma}, \sigma\rangle$ have a nonvanishing contribution. Thus, the Kondo cat coexists with the exchange-coupled RKKY considered before. With contemporary control over both the cavity and the dots levels, the Kondo cat is within experimental reach and can serve as a meter for the spin coherence length scales in the system [34]. This is the third key result of our work; we predict an exotic Kondo effect, where a nonlocal superposition of macroscopic Kondo effects arises. The Kondo cat formation fundamentally sets our system apart from standard double-dot systems [33].
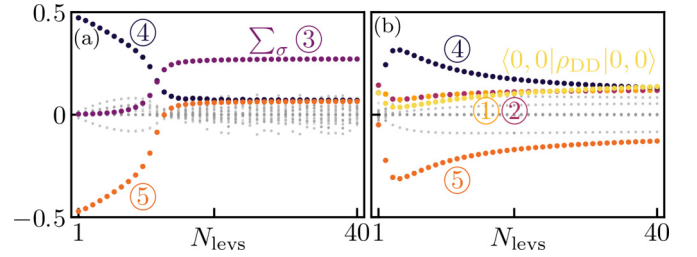

FIG. 3. *Crossovers between the (2) and (1) limits.* NRG-MPS tomography results of the cavity double-dot system as a function of the number of cavity energy levels N_{levs}, $\delta = 0.25U/N_{\text{levs}}$. As in Fig. 2, we highlight the elements with a contribution $|\langle s, s'|\rho_{\text{DD}}|s'', s'''\rangle| > 0.1$. (a) System (2) with $\epsilon_{\text{L}} = \epsilon_{\text{R}} = -U/2$, $\tilde{t}_{\text{D}} = 0.15U$. (b) System (2) with $\epsilon_{\text{L}} = \epsilon_{\text{R}} = U$, $\tilde{t}_{\text{D}} = 0.15U$. We use NRG chain length $N = 40$ and MPS bond dimension $D = 300$. (Other parameters and markers are as in Fig. 2).

Dependence on the central region's level spacing. We observed two distinct effects associated with the coherent dot-dot coupling as mediated by the cavity [case (2)]: the cavity-mediated RKKY and Kondo cat regimes. We now examine the crossover between the limiting scenarios (2) and (1) in these regimes, see Fig. 3. We set equidistant cavity levels $N_{\text{levs}} = 1, 2, \ldots$, where the spacing is determined by $\delta = 0.25U/N_{\text{levs}}$ [55]. In Fig. 3(a), we consider the regime, where for $N_{\text{levs}} = 1$ the cavity-mediated RKKY effect (iv) is observed. For increasing cavity levels, we observe that the antiferromagnetic terms go toward zero. Concurrently, the ferromagnetic terms become more dominant. Therefore, we observe how the RKKY effect is suppressed by ferromagnetic superexchange, cf. Table I. Differently from the $\delta \approx 0$ case, the antiferromagnetic order parameters are negligible. In Fig. 3(b), we consider the regime, where for $N_{\text{levs}} = 1$ the Kondo cat (v) is observed. For increasing cavity levels, we observe that the configuration of the Kondo-cat-like parameters is rapidly suppressed. Concurrently, the configuration of the RKKY-like interaction becomes dominant. The Kondo cat effect is suppressed by the RKKY interaction, cf. Table I. Notably, the observed crossovers occur at $N_{\text{levs}} < 20$ for both regimes, which is significantly lower than in the continuous limit $N_{\text{levs}} \to \infty$ of system (1).

Conclusion. We find a rich variety of many-body states within a double-dot system, with a particular focus on the competition of Kondo with RKKY-like effects and predict an exotic nonlocal Kondo impurity. We demonstrate the potential of tomography analysis [41] in understanding and distinguishing between the different strongly correlated states. To accomplish this, we apply and expand the NRG-MPS methodology to encompass complex multi-impurity multireservoir setups. Throughout the work, we employ typical values for the coupling parameters that enable the experimental exploration of the RKKY regime and detection of the Kondo cat regimes in the cavity-double-dot setup [34,35]. The coupling of quantum dots to cavity modes potentially extends to silicon [56] or bilayer graphene [57,58] devices. Future work will focus on finding transport observables sensitive to the different many-body ground states. Our findings motivate the potential application of Kondo-box-like-double-dot systems

[1] D. Loss and D. P. DiVincenzo, Quantum computation with quantum dots, Phys. Rev. A **57**, 120 (1998).

[2] G. Burkard, T. D. Ladd, A. Pan, J. M. Nichol, and J. R. Petta, Semiconductor spin qubits, Rev. Mod. Phys. **95**, 025003 (2023).

[3] L. I. Glazman, F. W. J. Hekking, and A. I. Larkin, Kondo effect in quantum dots, in *Statistical and Dynamical Aspects of Mesoscopic Systems*, Lecture Notes in Physics, edited by D. Reguera, J. M. Rubí, G. Platero, and L. L. Bonilla (Springer, Berlin, Heidelberg, 2000), pp. 16–26.

[4] P. Coleman, *Introduction to Many-Body Physics* (Cambridge University Press, Cambridge, 2015).

[5] J. Kondo, Resistance minimum in dilute magnetic alloys, Prog. Theor. Phys. **32**, 37 (1964).

[6] A. A. Abrikosov, Magnetic impurities in nonmagnetic metals, Sov. Phys. Usp. **12**, 168 (1969).

[7] T. K. Ng and P. A. Lee, On-site coulomb repulsion and resonant tunneling, Phys. Rev. Lett. **61**, 1768 (1988).

[8] A. Kawabata, On the electron transport through a quantum dot, J. Phys. Soc. Jpn. **60**, 3222 (1991).

[9] M. A. Ruderman and C. Kittel, Indirect exchange coupling of nuclear magnetic moments by conduction electrons, Phys. Rev. **96**, 99 (1954).

[10] T. Kasuya, A theory of metallic ferro- and antiferromagnetism on Zener's model, Prog. Theor. Phys. **16**, 45 (1956).

[11] K. Yosida, Magnetic properties of Cu-Mn alloys, Phys. Rev. **106**, 893 (1957).

[12] C. Jayaprakash, H. R. Krishna-murthy, and J. W. Wilkins, Two-impurity Kondo problem, Phys. Rev. Lett. **47**, 737 (1981).

[13] B. A. Jones, C. M. Varma, and J. W. Wilkins, Low-temperature properties of the two-impurity Kondo Hamiltonian, Phys. Rev. Lett. **61**, 125 (1988).

[14] Y. Utsumi, J. Martinek, P. Bruno, H. Imamura, and S. Maekawa, RKKY interaction between two quantum dots embedded in an Aharonov-Bohm ring, in *Realizing Controllable Quantum States* (World Scientific, Singapore, 2005), pp. 439–444.

[15] M. G. Vavilov and L. I. Glazman, Transport spectroscopy of Kondo quantum dots coupled by RKKY interaction, Phys. Rev. Lett. **94**, 086805 (2005).

[16] L. G. G. V. Dias da Silva, E. Vernek, K. Ingersent, N. Sandler, and S. E. Ulloa, Spin-polarized conductance in double quantum dots: Interplay of Kondo, Zeeman and interference effects, Phys. Rev. B **87**, 205313 (2013).

[17] A. Bayat, S. Bose, P. Sodano, and H. Johannesson, Entanglement probe of two-impurity Kondo physics in a spin chain, Phys. Rev. Lett. **109**, 066403 (2012).

[18] L. Pan, Y. Wang, Z. Li, J. Wei, and Y. Yan, Kondo effect in double quantum dots with ferromagnetic RKKY interaction, J. Phys.: Condens. Matter **29**, 025601 (2017).

[19] I. Weymann, R. Chirla, P. Trocha, and C. P. Moca, SU(4) Kondo effect in double quantum dots with ferromagnetic leads, Phys. Rev. B **97**, 085404 (2018).

[20] A. V. Parafilo and M. N. Kiselev, Tunable RKKY interaction in a double quantum dot nanoelectromechanical device, Phys. Rev. B **97**, 035418 (2018).

[21] C. Piermarocchi, P. Chen, L. J. Sham, and D. G. Steel, Optical RKKY interaction between charged semiconductor quantum dots, Phys. Rev. Lett. **89**, 167402 (2002).

[22] D. P. Divincenzo, Topics in quantum computers, in *Mesoscopic Electron Transport*, NATO ASI Series, edited by L. L. Sohn, L. P. Kouwenhoven, and G. Schön (Springer Netherlands, Dordrecht, 1997), pp. 657–677.

[23] T. T. Ong and B. A. Jones, Generalized Schrieffer-Wolff transformation of the two-impurity Kondo model, Europhys. Lett. **93**, 57004 (2011).

[24] S.-R. E. Yang, J. Schliemann, and A. H. MacDonald, Quantum-Hall quantum bits, Phys. Rev. B **66**, 153302 (2002).

[25] V. W. Scarola, J. K. Jain, and E. H. Rezayi, Possible pairing-induced even-denominator fractional quantum Hall effect in the lowest Landau level, Phys. Rev. Lett. **88**, 216804 (2002).

[26] S. J. Elman, S. D. Bartlett, and A. C. Doherty, Long-range entanglement for spin qubits via quantum Hall edge modes, Phys. Rev. B **96**, 115407 (2017).

[27] K. D. Petersson, L. W. McFaul, M. D. Schroer, M. Jung, J. M. Taylor, A. A. Houck, and J. R. Petta, Circuit quantum electrodynamics with a spin qubit, Nature (London) **490**, 380 (2012).

[28] H. Toida, T. Nakajima, and S. Komiyama, Vacuum rabi splitting in a semiconductor circuit QED system, Phys. Rev. Lett. **110**, 066802 (2013).

[29] Y.-Y. Liu, K. D. Petersson, J. Stehlik, J. M. Taylor, and J. R. Petta, Photon emission from a cavity-coupled double quantum dot, Phys. Rev. Lett. **113**, 036801 (2014).

[30] G.-W. Deng, D. Wei, J. R. Johansson, M.-L. Zhang, S.-X. Li, H.-O. Li, G. Cao, M. Xiao, T. Tu, G.-C. Guo, H.-W. Jiang, F. Nori, and G.-P. Guo, Charge number dependence of the dephasing rates of a graphene double quantum dot in a circuit QED architecture, Phys. Rev. Lett. **115**, 126804 (2015).

[31] A. Stockklauser, P. Scarlino, J. V. Koski, S. Gasparinetti, C. K. Andersen, C. Reichl, W. Wegscheider, T. Ihn, K. Ensslin, and A. Wallraff, Strong coupling cavity QED with gate-defined double quantum dots enabled by a high impedance resonator, Phys. Rev. X **7**, 011030 (2017).

[32] S.-S. Gu, S. Kohler, Y.-Q. Xu, R. Wu, S.-L. Jiang, S.-K. Ye, T. Lin, B.-C. Wang, H.-O. Li, G. Cao, and G.-P. Guo, Probing two driven double quantum dots strongly coupled to a cavity, Phys. Rev. Lett. **130**, 233602 (2023).

[33] N. J. Craig, J. M. Taylor, E. A. Lester, C. M. Marcus, M. P. Hanson, and A. C. Gossard, Tunable nonlocal spin control in a coupled-quantum dot system, Science **304**, 565 (2004).

[34] G. Nicolí, M. S. Ferguson, C. Rössler, A. Wolfertz, G. Blatter, T. Ihn, K. Ensslin, C. Reichl, W. Wegscheider, and O. Zilberberg, Cavity-mediated coherent coupling between distant quantum dots, Phys. Rev. Lett. **120**, 236801 (2018).

[35] C. Rössler, D. Oehri, O. Zilberberg, G. Blatter, M. Karalic, J. Pijnenburg, A. Hofmann, T. Ihn, K. Ensslin, C. Reichl, and W. Wegscheider, Transport spectroscopy of a spin-coherent dot-cavity system, Phys. Rev. Lett. **115**, 166603 (2015).

[36] M. S. Ferguson, D. Oehri, C. Rössler, T. Ihn, K. Ensslin, G. Blatter, and O. Zilberberg, Long-range spin coherence in a strongly coupled all-electronic dot-cavity system, Phys. Rev. B **96**, 235431 (2017).

[37] L. G. G. V. Dias da Silva, C. H. Lewenkopf, E. Vernek, G. J. Ferreira, and S. E. Ulloa, Conductance and Kondo interference beyond proportional coupling, Phys. Rev. Lett. **119**, 116801 (2017).

[38] C. Gold, B. A. Bräm, M. S. Ferguson, T. Krähenmann, A. Hofmann, R. Steinacher, K. R. Fratus, C. Reichl, W. Wegscheider, D. Weinmann, K. Ensslin, and T. Ihn, Imaging signatures of the local density of states in an electronic cavity, Phys. Rev. Res. **3**, L032005 (2021).

[39] J. A. Katine, M. A. Eriksson, A. S. Adourian, R. M. Westervelt, J. D. Edwards, A. Lupu-Sax, E. J. Heller, K. L. Campman, and A. C. Gossard, Point contact conductance of an open resonator, Phys. Rev. Lett. **79**, 4806 (1997).

[40] J. S. Hersch, M. R. Haggerty, and E. J. Heller, Diffractive orbits in an open microwave billiard, Phys. Rev. Lett. **83**, 5342 (1999).

[41] L. Stocker, S. H. Sack, M. S. Ferguson, and O. Zilberberg, Entanglement-based observables for quantum impurities, Phys. Rev. Res. **4**, 043177 (2022).

[42] P. W. Anderson, Localized magnetic states in metals, Phys. Rev. **124**, 41 (1961).

[43] W. B. Thimm, J. Kroha, and J. von Delft, Kondo box: A magnetic impurity in an ultrasmall metallic grain, Phys. Rev. Lett. **82**, 2143 (1999).

[44] K. G. Wilson, The renormalization group: Critical phenomena and the Kondo problem, Rev. Mod. Phys. **47**, 773 (1975).

[45] H. R. Krishna-murthy, J. W. Wilkins, and K. G. Wilson, Renormalization-group approach to the Anderson model of dilute magnetic alloys. II. Static properties for the asymmetric case, Phys. Rev. B **21**, 1044 (1980).

[46] H. R. Krishna-murthy, J. W. Wilkins, and K. G. Wilson, Renormalization-group approach to the Anderson model of dilute magnetic alloys. I. Static properties for the symmetric case, Phys. Rev. B **21**, 1003 (1980).

[47] R. Bulla, T. A. Costi, and T. Pruschke, Numerical renormalization group method for quantum impurity systems, Rev. Mod. Phys. **80**, 395 (2008).

[48] H. Saberi, A. Weichselbaum, and J. von Delft, Matrix-product-state comparison of the numerical renormalization group and the variational formulation of the density-matrix renormalization group, Phys. Rev. B **78**, 035124 (2008).

[49] A. Weichselbaum, F. Verstraete, U. Schollwöck, J. I. Cirac, and J. von Delft, Variational matrix product state approach to quantum impurity models, Phys. Rev. B **80**, 165117 (2009).

[50] J. R. Schrieffer and P. A. Wolff, Relation between the Anderson and Kondo Hamiltonians, Phys. Rev. **149**, 491 (1966).

[51] H. Bruus and K. Flensberg, *Many-Body Quantum Theory in Condensed Matter Physics: An Introduction* (Oxford University Press, Oxford, 2004).

[52] See Supplemental Material at http://link.aps.org/supplemental/10.1103/PhysRevResearch.6.L022058 for details on: (1) NRG Hamiltonian decomposition, (2) Schrieffer-Wolff transformation, (3) Schrieffer-Wolff transformation of the single impurity Anderson model, (4) Exact diagonalization and Schrieffer-Wolff transformation of the closed cavity-double-dot system, (5) Variational Matrix Product State algorithm for degenerate states.

[53] In Ref. [23], fourth-order correction terms were derived using the Schrieffer-Wolff transformation. They obtain a RKKY interaction and a superexchange interaction term. In the parameter regime of Fig. 2(b), the superexchange coupling coefficient is negative, favoring a ferromagnetic effect.

[54] In the case of a large central dot [33], a phase transition is analytically predicted [62,63].

[55] This choice is motivated the fact that we have $\epsilon_c = 0.75U$ and aim to keep the cavity levels within the energy bandwidth of the NRG lead $\mathcal{D} = [-U, U]$.

[56] B. Weber, Y. H. M. Tan, S. Mahapatra, T. F. Watson, H. Ryu, R. Rahman, L. C. L. Hollenberg, G. Klimeck, and M. Y. Simmons, Spin blockade and exchange in Coulomb-confined silicon double quantum dots, Nat. Nanotechnol. **9**, 430 (2014).

[57] A. Kurzmann, Y. Kleeorin, C. Tong, R. Garreis, A. Knothe, M. Eich, C. Mittag, C. Gold, F. K. de Vries, K. Watanabe, T. Taniguchi, V. Fal'ko, Y. Meir, T. Ihn, and K. Ensslin, Kondo effect and spin-orbit coupling in graphene quantum dots, Nat. Commun. **12**, 6004 (2021).

[58] L. Banszerus, A. Rothstein, E. Icking, S. Möller, K. Watanabe, T. Taniguchi, C. Stampfer, and C. Volk, Tunable interdot coupling in few-electron bilayer graphene double quantum dots, Appl. Phys. Lett. **118**, 103101 (2021).

[59] P. Mohanty, E. M. Q. Jariwala, and R. A. Webb, Intrinsic decoherence in mesoscopic systems, Phys. Rev. Lett. **78**, 3366 (1997).

[60] G. Xu, C. Broholm, Y.-A. Soh, G. Aeppli, J. F. DiTusa, Y. Chen, M. Kenzelmann, C. D. Frost, T. Ito, K. Oka, and H. Takagi, Mesoscopic phase coherence in a quantum spin fluid, Science **317**, 1049 (2007).

[61] M. Fishman, S. White, and E. Stoudenmire, The ITensor software library for tensor network calculations, SciPost Phys. Codebases, 4 (2022).

[62] I. Affleck and A. W. W. Ludwig, Exact critical theory of the two-impurity Kondo model, Phys. Rev. Lett. **68**, 1046 (1992).

[63] D. F. Mross and H. Johannesson, Two-impurity Anderson model at quantum criticality, Phys. Rev. B **78**, 035449 (2008).